MJFAS
Malaysian Journal of Fundamental and Applied Sciences

Yasin *et al.* | Malaysian Journal of Fundamental and Applied Sciences, Vol. 19 (2023) 142-153

RESEARCH ARTICLE

Effect of Wall Oscillation Period on Fluid Flow in Branched Channel with a Moving Indentation

Roliza Md Yasin[a,*], Erwan Hafizi Kasiman[b], Norsarahaida Saidina Amin[c], Airil Yasreen Mohd Yassin[d], Ahmad Kueh Beng Hong[e], Norzieha Mustapha[a]

[a]Faculty of Computer and Mathematical Sciences, Universiti Teknologi MARA Cawangan Kelantan, Kampus Machang, 18500 Machang, Kelantan, Malaysia; [b]Department of Hydraulic and Hydrology, Faculty of Civil Engineering, Universiti Teknologi Malaysia, 81310 UTM Johor Bahru, Johor, Malaysia; [c]Department of Mathematical Sciences, Faculty of Science, Universiti Teknologi Malaysia, 81310 UTM Johor Bahru, Johor, Malaysia; [d]School of Energy, Geoscience, Infrastructure and Society, Heriot-Watt University Malaysia; [e]Department of Civil Engineering, Faculty of Engineering, Universiti Malaysia Sarawak, Malaysia

Abstract The numerical simulation of two-dimensional fluid flow in T-shaped and Y-shaped channels having a single moving indented wall is performed by the finite element method in the Arbitrary Lagrangian-Eulerian frame. The motion of the indented wall is defined as a hyperbolic function, and it is located at a small segment at the bottom wall in the parent channel. The smallest value of the wall oscillation period causes the waviest core flow in the main channel, resulting in bigger vortices and greater flow separation region in the branches, especially during the outward indentation motion. This flow disturbance pattern is found more severe in T-channel as compared to that of in Y-channel.

Keywords: ALE-FEM, bifurcation, moving indented wall.

Nomenclature

Δt	-	time increment
ρ_f	-	fluid density
d	-	indentation height at the time, t
d_{max}	-	maximum indentation height
d_x	-	horizontal mesh displacement
d_y	-	vertical displacement
$\mathbf{d_m}$	-	mesh displacements vector
${}^{n+1}\mathbf{d_m}$	-	mesh displacements vector at the time $t = n+1$
h	-	channel height
L	-	characteristic length of the channel
L1	-	distance between the inlet and the left end of the indentation
L2	-	indentation length
L3	-	distance between the outlet and the right end of the indentation
p	-	pressure of fluid
Re	-	Reynolds number

***For correspondence:**
roliza927@uitm.edu.my

Received: 26 June 2022
Accepted: 15 Feb. 2023

10.11113/mjfas.v19n2.2659

St	-	Strouhal number
t	-	time
*t**	-	the ratio between time and oscillation period
T_0	-	oscillation period
u_f	-	the horizontal velocity of the fluid
u_g	-	the horizontal velocity of mesh
U_e	-	characteristic velocity
$\mathbf{U}$	-	fluid velocity vector
${}^{n+1}\mathbf{U}$	-	fluid velocity vector at time *t = n+1*
v_f	-	vertical velocity of the fluid
v_g	-	vertical velocity of mesh
$\mathbf{w}$	-	mesh velocity vector
${}^{n+1}\mathbf{w}$	-	mesh velocity vector at time *t = n+1*
x_1, x_2, x_3	-	parameters of the indented wall
(x, y)	-	local/Cartesian coordinate system

Introduction

The fluid flow simulation work in a channel with a moving indented wall started almost forty years ago. The first effort of [14] involved experimental work where their findings became the validation case for many numerical works later. All the simulation works considered fluid dynamics in deformable domains and is significantly important in reflecting the actual fluid flow. One typical example is the flow of blood in a diseased artery which is called atherosclerosis. This condition might cause distinct effects on different patients depending on the location of the constriction and its severity level.

In general, the works on simulating the fluid flow in a channel having a moving indentation wall can be categorized into two types i.e horizontal (axial) or vertical (radial) movement. [9] and [16] considered the axial motion, mimicking the rolling manipulation of traditional Chinese medical massage. But, the use of vertical moving indentation is more commonly found in previous studies [2, 4, 5, 7, 13, 18]. It is found that [2, 4, 5, 7] had validated either the proposed method or the discretized model with [4]. [4] was the first numerical simulation study of two-dimensional fluid flow in a channel having vertical indented wall movement. They described the geometry of the indented wall by a hyperbolic tangent function following the experimental work of [14] and employed the finite difference technique. Even though the domain of fluid flow changes in time, the Eulerian frame was retained with the adoption of extra efforts such as variable transformation [4, 5, 15] and dynamic mesh model [2].

The alternative concept defines fluid mechanics in a deformable domain using the Arbitrary Langrangian-Eulerian (ALE) frame. In this frame, arbitrary movement of interior mesh is allowed but it is independent of the fluid velocity. As for the nodes located on the moving boundary, they follow the boundary motion strictly. This concept is commonly used in handling fluid-structure interaction problems. [22] applied the serial and parallel ALE, incompressible flow solvers, to the aerodynamic computation of micro air vehicles. The work involved a series of validation cases of two-sided, lid-driven cavity flow, flows passing through a collapsible channel, and over an oscillating circular cylinder. The adoption of ALE in simulating the fluid flow in moving indented walls, using spectral element and solution-dependent weighted least squares are found in [13] and [18] respectively.

There are few studies on the effect of a few parameters or factors of fluid flow in a deformable channel. [3] investigated the effect of gravitational force on pressure drop in a bifurcated mild stenosed artery. They observed high pressure drop in the more severe stenosed artery. As a uniform external magnetic field was exposed to a bifurcated artery with overlapping stenosis, [21] investigated the effects of two dimensionless numbers on the fluid's velocity and pressure. They found that Hartmann number influence became less prominent as compared to Reynolds number at the daughter branch. Meanwhile, the former showed a more significant effect at the daughter branch having no constriction compared to the constriction area at the mother artery. Another frequently observable effect involves the chemical reaction in the circulatory system [12, 20]. [12] found that the dispersion of drugs and nutrients in the blood flow happened at a slow shear rate through narrow arteries. [20] concluded that the penetration of chemical substances into the vessel wall led to changes in volume and wall mechanical properties.

There are few analytical and numerical works investigating the spanwise traveling waves of wall induction motions in a two-dimensional turbulent channel flow [1, 17, 19]. The fluid is modeled as a

superposition of the Pouiseullie flow and the Stokes layer and the temporal-forced wall motions are categorized as oscillatory [1, 17] and deformable [19]. The studies observed a considerable drag reduction over the region where oscillation occurs depending on a few parameters such as Reynold number, the period, and the amplitude of the wall oscillation. To date, the work on the effect of varying the wall oscillating period on the fluid flow in a simplified branched channel is less documented. The oscillation period of the moving wall is defined as the time taken for the wall to complete its cycle. It means, the time taken by the wall to recede to the same position for the first time. A smaller value of the oscillation period means faster wall movement. In blood flow problems, it represents the movement of stenosis in a diseased artery. In a patient having stenosis, a slightly abnormal heart pumping activity might cause irregular blood flow which eventually would cause severe effects and be life-threatening.

The present study aims to investigate any possible flow disturbance due to the motion of a single indented wall in two types of branched channels. Here, the simulation work of [11] on fluid flow in the Y-channel and T-channel is being extended to investigate the effect of different values of the oscillation period. The second section of this report presents the domain and mathematical model of the problem. Here, we consider two branched channels of T-channel and Y-channel with a single moving indented wall located at the bottom of both main channels. The third section discusses the procedure for solving the mathematical model involving the finite element approach in the ALE frame using Matlab coding. The fourth section presents the preliminary work in performing the procedure by solving the fluid flow in a straight channel with the same indented wall. The finding is consistent with Ben-Mansour [2] and validates the numerical procedure in solving the fluid flow problem. Next, the fifth section discusses the fluid flow behavior in the two branched channels for several different values of the oscillation period of the moving wall. Finally, the sixth section concludes the findings regarding the effect of the wall oscillation period and the fluid flow in the two branched channels.

Mathematical Formulation

The present problem is being formulated by first defining the geometrical domain for the two branched channels in which the fluid flows inside them. Then, the dynamical behaviour of the fluid is then explained by the three governing equations with the corresponding initial and boundary conditions.

Geometry profile

There are two geometrical domains considered in this present work as shown in Figure 1.

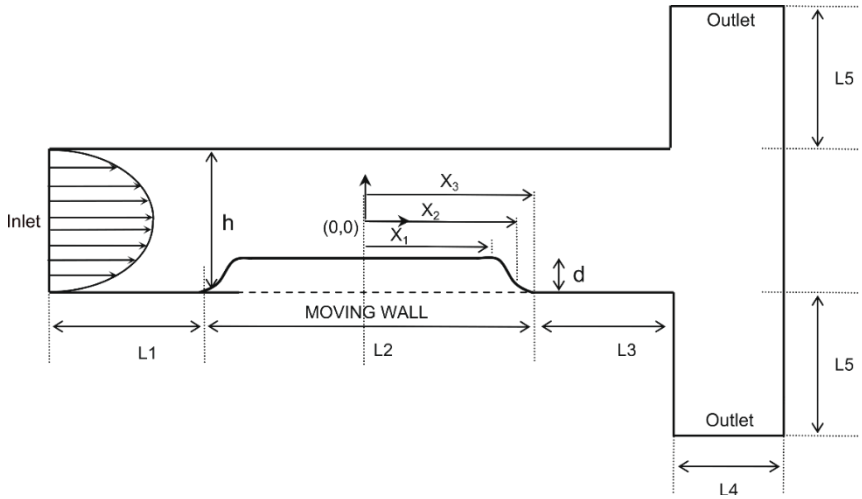

(A)

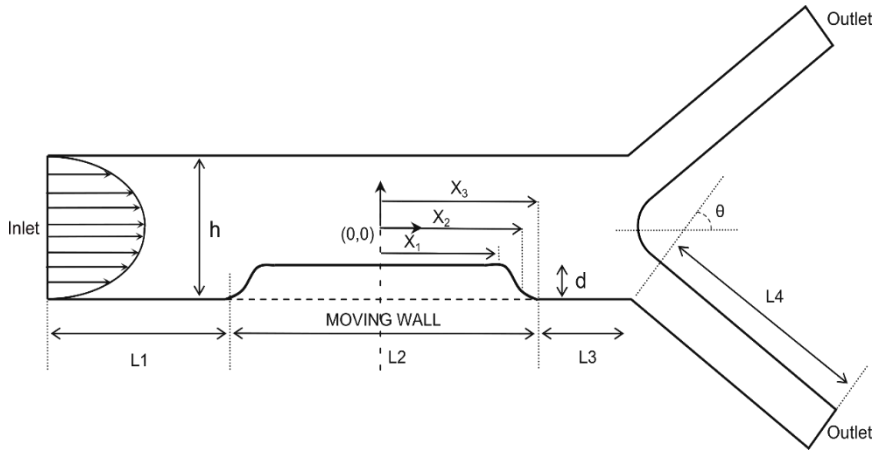

(B)

Figure 1. The geometry of a single indented moving wall in an (A) T-channel; (B) Y-channel

The half configuration of the indented wall is algebraically represented in equation (1) [6].

$$d(x,t)=\begin{cases} 0.5d_{\max}\,h\left(1-\cos\left(\dfrac{2\pi t}{T_0}\right)\right) & ;\ x_0 \le x \le x_1 \\ 0.25d_{\max}\left(1-\cos\left(\dfrac{2\pi t}{T_0}\right)\right)\left(1-\tanh\left(\alpha\left(x-x_2\right)\right)\right) & ;\ x_1 \le x \le x_3 \\ 0 & ;\ x \ge x_3 \end{cases} \quad (1)$$

The geometrical parameters involved are h = 0.01m, x_1= 4h, x_2 = 0.5(x_1 + x_3), x_3 = 6.5, α =4.14, d_{max} = 0.0038 m. Other parameters are ρ = 1000 kgm^{-3}, U_e = 0.01 ms^{-1}, L = 0.01 m, μ =0.000197 kgm^{-1}s^{-1} and T_0 = 27 s. They are the density, characteristic velocity, characteristic length, dynamic viscosity, and oscillation period respectively. The two dimensionless numbers are Reynolds number, Re = ρUeL/μ = 507, and Strouhal number, St = L/(UeT_0) = 0.037. Other parameters are L1 = 0.03 m, L2 = 0.04 m, L3 = 0.05 m, L4 = 0.01 m, L5 = 0.05 m for the T-channel. As for the Y-channel, the parameter values are L1 = 0.05 m, L2 = 0.04 m, L3 = 0.01 m, L4 = 0.04 m and θ = 30^o.

Mathematical model

This two-dimensional incompressible, isothermal fluid problem is described in an Arbitrary Lagrangian-Eulerian frame and the governing equations are given in equations (2), (3) and (4) :

$$\frac{\partial u_f}{\partial x}+\frac{\partial v_f}{\partial y}=0 \quad (2)$$

$$\left(\frac{\partial u_f}{\partial t}+\left(u_f-u_g\right)\frac{\partial u_f}{\partial x}+\left(v_f-v_g\right)\frac{\partial u_f}{\partial y}\right)=\frac{1}{\rho_f}\left(-\frac{\partial p}{\partial x}+\mu\frac{\partial^2 u_f}{\partial x^2}+\mu\frac{\partial^2 u_f}{\partial y^2}\right) \quad (3)$$

$$\left(\frac{\partial v_f}{\partial t}+\left(u_f-u_g\right)\frac{\partial v_f}{\partial x}+\left(v_f-v_g\right)\frac{\partial v_f}{\partial y}\right)=\frac{1}{\rho_f}\left(-\frac{\partial p}{\partial y}+\mu\frac{\partial^2 v_f}{\partial x^2}+\mu\frac{\partial^2 v_f}{\partial y^2}\right) \quad (4)$$

Fluid horizontal velocity, vertical velocity, and pressure are $u_f = u_f(x,y,t)$, $v_f = v_f(x,y,t)$ and $p = p(x,y,t)$. u_g and v_g are mesh horizontal and vertical velocities respectively. The two parameters are

fluid density, ρ_f and dynamic viscosity, μ. The initial values of u_f , v_f and *p* are obtained by solving the two-dimensional incompressible Stokes flow problem whereas u_g and v_g are set as zeros. At the inlet, the flow is assumed as parabolic whilst a zero-pressure value is set at the outlet. No slip boundary condition, $(u_f = u_g, v_f = v_g)$ is imposed at the top and bottom walls but the values differ depending on the deformability of the wall. Zero values of fluid pressure, velocities, and mesh velocities are assigned at the non-deformable boundaries but the boundary condition at the deforming boundaries is given in equation (5).

$$v_f = v_g = \begin{cases} 0.5 d_{\max} h\left(\frac{2\pi}{T_0}\right)\sin\left(\frac{2\pi}{T_0}\right) & ;\ 0 \le x \le x_1 \\ 0.5 d_{\max} h\left(\frac{2\pi}{T_0}\right)\sin\left(\frac{2\pi}{T_0}\right)\left(1-\tanh\left(\alpha\left(x-x_2\right)\right)\right) & ;\ x_1 \le x \le x_3 \\ 0 & ;\ x \ge x_3 \end{cases} \quad (5)$$

As the present problem defines the dynamics of fluid in the ALE frame, the mesh velocities at each instantaneous time, *n*+1 i.e u_g^{n+1} and v_g^{n+1} must be assigned first before performing the procedure. The present study adopts the pseudo-structural technique in defining the mesh motion. It assumes the mesh motion to imitate the mechanics of one structural element i.e plane-stress element.

Method of Solution

The solution to this fluid flow problem includes the discretization of the domain of the problem and the governing equations. The problem domains as described in Figure 1 are discretized by using a biquadratic quadrilateral finite element. The process of solving the mathematical model defined in the previous section is summarized in Figure 2. The main steps involved are:

Step 1: Solve the Stokes equations using the standard Galerkin technique.

The solution to the equations in vector form is $\mathbf{U}_{Stokes} = (u_{Stokes}, v_{Stokes}, p_{Stokes})$. Then, it is taken as the initial values in solving the Navier-Stokes equations

Step 2: Solve the plane stress equation with the boundary condition defined in equation (5) using the standard Galerkin technique.

The solution of the equation in vector form is ${}^1\mathbf{d_m} = ({}^1d_x\ ,\ {}^1d_y)$ where ${}^1d_x$ is the mesh horizontal displacement and ${}^1d_y$ is the mesh vertical displacement for the first iteration. The displacement values are used to calculate the mesh horizontal and vertical velocities as shown in equation (6) with zero initial values.

$${}^{n+1}u_g = \frac{{}^{n+1}d_x - {}^{n}d_x}{\Delta t}, \quad {}^{n+1}v_g = \frac{{}^{n+1}d_y - {}^{n}d_y}{\Delta t} \quad (6)$$

Hence, the mesh velocity in vector form is ${}^1\mathbf{w} = ({}^1u_g\ ,\ {}^1v_g\ )$.

Step 3: Solve the Navier-Stokes equations (2), (3), and (4) with initial conditions ${}^0\mathbf{U} = \mathbf{U}_{Stokes}$ using the Bubnov-Galerkin technique

Euler backward technique is used in discretizing the time derivative term in the equations. The solution of the equation at the first iteration is ${}^1\mathbf{U}$ and the values are used to obtain the solution for the next time step.

Step 4: Steps 2 and 3 are repeated with the updated values in the recent time step. The repetition continues until the desired time is achieved.

The iteration process is performed by Matlab coding.

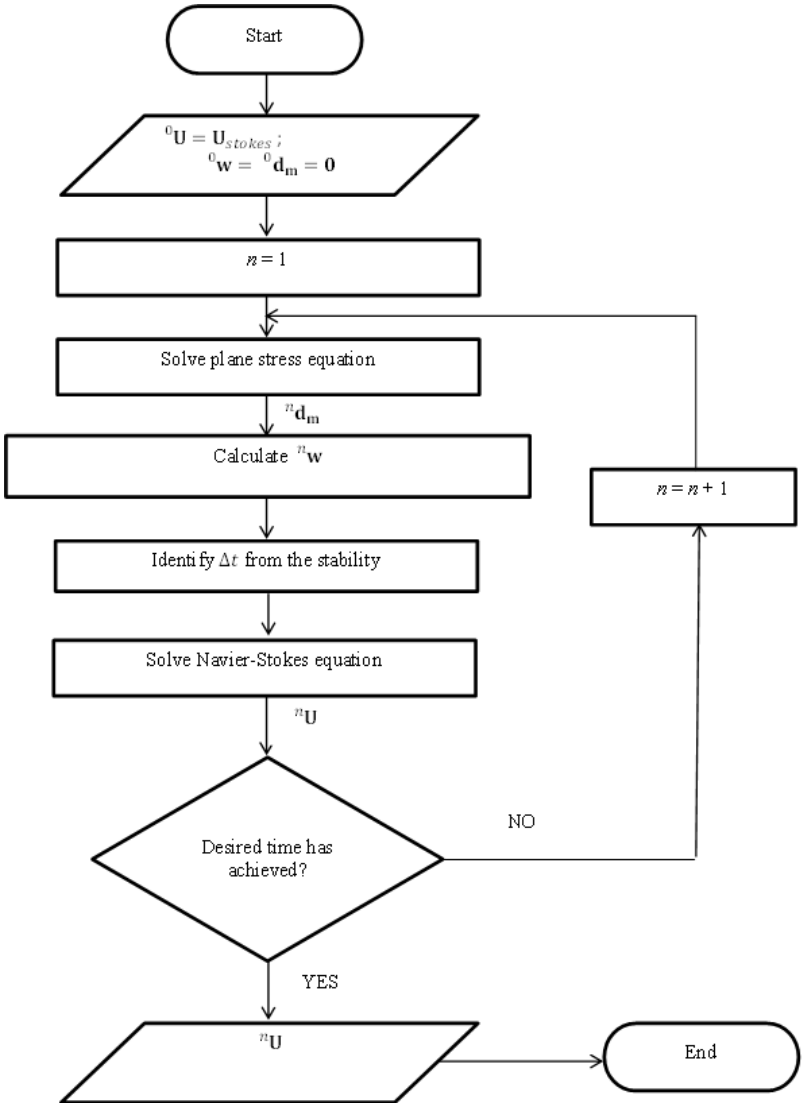

Figure 2. Solution procedure

The stability condition for ALE-FEM convective formulation is shown in equation (7) [8].

$$\Delta t \leq \frac{2}{\max\left|\nabla .^{n+1}\mathbf{w}\right|} \tag{7}$$

This time step condition must be calculated before solving equations (2)-(4) for each time, *t*. The divergence of mesh velocity at *n*+1 time is approximated at each time iteration.

Model Validation

The use of the ALE-FEM approach in solving this present fluid problem is validated by reproducing the work of [15]. They investigated the pattern of fluid flow in a straight channel having a single indented moving wall as shown in Figure 3.

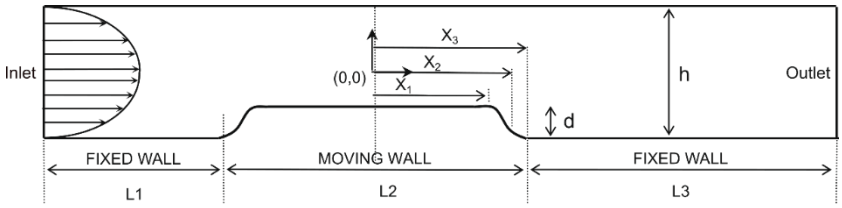

Figure 3. A straight channel with a single indented wall

Figure 4 shows the horizontal velocity profiles at *x* = 0 m (the midpoint of the indentation) for two different instantaneous times.

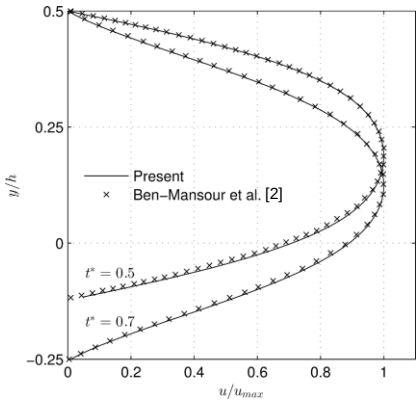

Figure 4. Horizontal velocity profile at x = 0 m

The time is defined by a new parameter, ranging between 0 and 1, whereas all the ordinates in the figure are defined as the normalized height of the channel. Figure 4 shows that the present two horizontal profiles are overlapped with the ones obtained by [2]. At the midpoint of the indented wall, fully developed flow is observed during the maximum indentation, $d = d_{\max}$ which is at $t^* = 0.5$. As the indented wall recedes $(t^* > 0.5)$, the flow shape becomes less parabolic in a gradual manner.

Results and Discussion

Three different values of oscillation periods, T_0 are applied to the mathematical models for the two branched channels, which are 5 seconds, 15 seconds, and 30 seconds. The motion of the indented wall is the fastest for T_0 = 5s as compared to the other two oscillation periods. The solutions to the mathematical models are analyzed by investigating the velocity distribution of the fluid flow and the wall shear stress (WSS) distribution along the channel wall. This report highlights the significant behavior of the fluid flow at two instantaneous times, *t** = 0.5 and *t** = 0.7. The former represents the time whenever the indented wall experiences its maximum height whilst the latter denotes the time wall recedes to its initial position.

Fluid Flow in a T-channel

In general, the low-velocity magnitude occurs at several locations such as at the left walls of daughter channels and the apex of the channel in a complete time cycle. As the indented wall moves inward (*t** < 0.5), the velocity magnitude increases but it decreases as the indented wall recedes to its initial position (0.5 < *t** < 1.00).

10.11113/mjfas.v19n2.2659

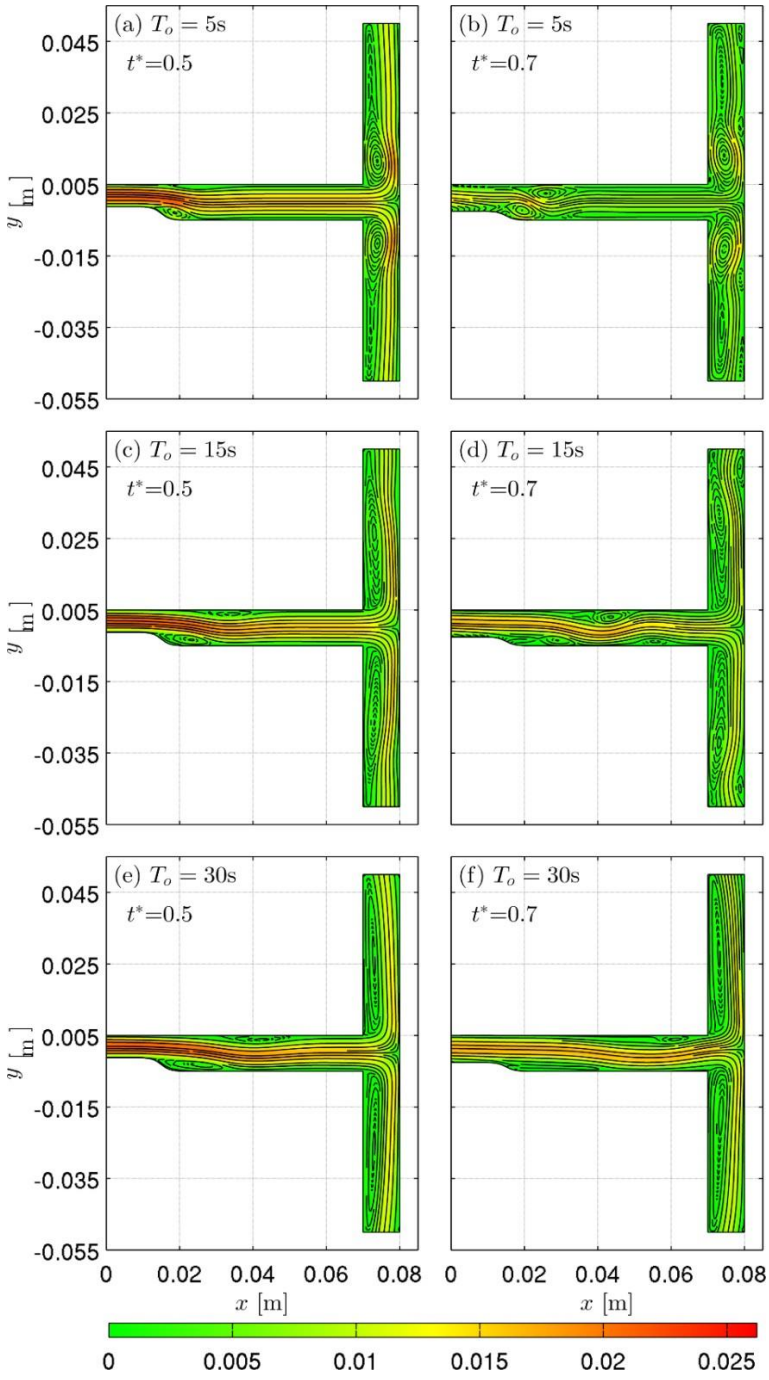

Figure 5. Streamlines and velocity plots for three different oscillation periods in T-channel

In Figure 5(a), (c) and (e) the flow pattern during maximum indentation (t^* = 0.5) shows a slight difference between the three different values of T_0. All the vortices become more stretchable as T_0 increases; which is close to the flow pattern at the initial time. In Figure 5(b), the wall is receding to the initial position and vortices and separation regions are formed along the right wall of the branches. Further, the two recirculatory regions on the left wall become greater in size. Figure 5(b), (d), and (f) show more stable flows are developed as T_0 increases. The wall shear stress (WSS) distributions along the bottom wall of the channel show significant differences throughout one complete time cycle. Figure 6 illustrates the differences which support the findings in Figure 5.

10.11113/mjfas.v19n2.2659

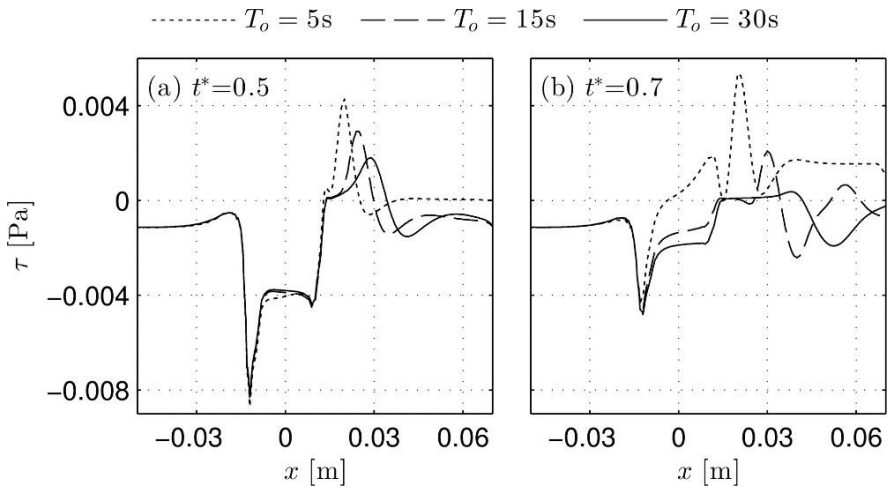

Figure 6. Wall shear stress distributions along the bottom wall in the deformable T-channel

In Figure 6(a) the shapes of WSS distribution for the three oscillation periods are similar with slight magnitude difference. The sign changes of WSS values occur twice (x ~ 0.02m and x ~ 0.03m) indicating the formation of one flow separation and reattachment region located at the right lee of the indentation. In Figure 6(b) and at T_0 = 5s, the flow separation is formed earlier i.e at x ~ -0.01m, and reattached at x ~ 0.02m; but it is immediately separated again. At T_0 = 30s, the flow separation and reattachment region occur with a small magnitude of WSS indicating the least flow disturbance among the three graph plots. In the meantime, at T_0 = 5s, the absolute value of WSS is found to be the highest at almost all locations along the bottom wall for the two instantaneous times.

Fluid Flow in a Y-channel

In general, low-velocity magnitude occurs along the top and bottom walls in the main channel and the two daughter channels in a complete time cycle. As the indented wall moves inward (t^* < 0.5), the velocity magnitude increases but it decreases as the indented wall recedes to its initial position (0.5 < t^* < 1.00). Figure 7 illustrates the flow pattern for three oscillation periods at two instantaneous times in a Y-channel. The Y-channel has an apex angle of sixty-degree and the ratio between the branch diameter and parent radius of one unit [10].

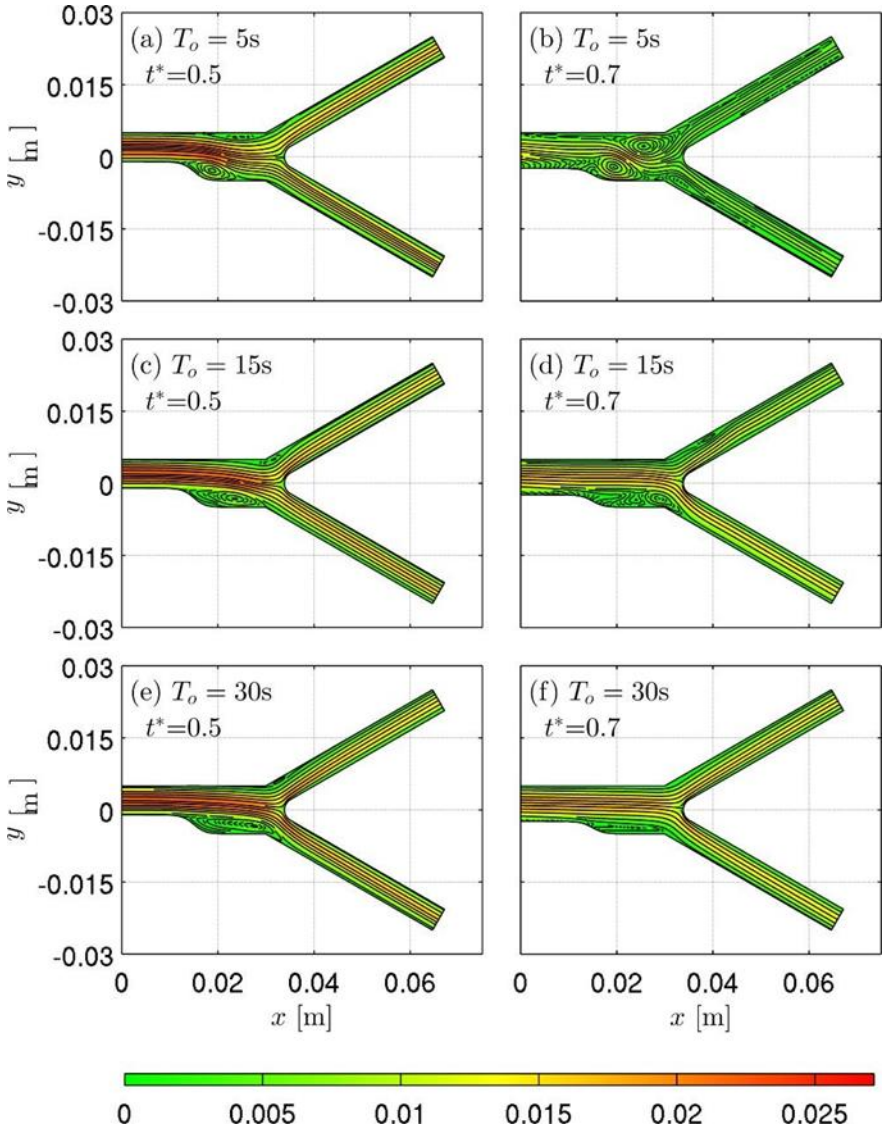

Figure 7. Streamlines and velocity plots for three different oscillation periods in Y-channel

In Figure 7 (a), (c), and (e), as the oscillation period increases, the main flow in the parent channel becomes less wavy causing the vortex in the parent channel to be stretched to the lower armpit of the channel. The vortex at the top wall moves downstream but does not show any obvious difference in size and shape. At the same time, the vortex at the bottom wall is stretched until it enters the lower branch at T_0 = 30s. At t^* = 0.7, the greatest flow disturbance is found at T_0 = 5s as shown in Figure 7(b). Meanwhile, Figure 7(f) has the least disturbance with the more stable flow and the existence of a reduced vortex at the bottom wall. Figure 8 shows the WSS distributions along the bottom wall for the three oscillation periods at two instantaneous times.

10.11113/mjfas.v19n2.2659

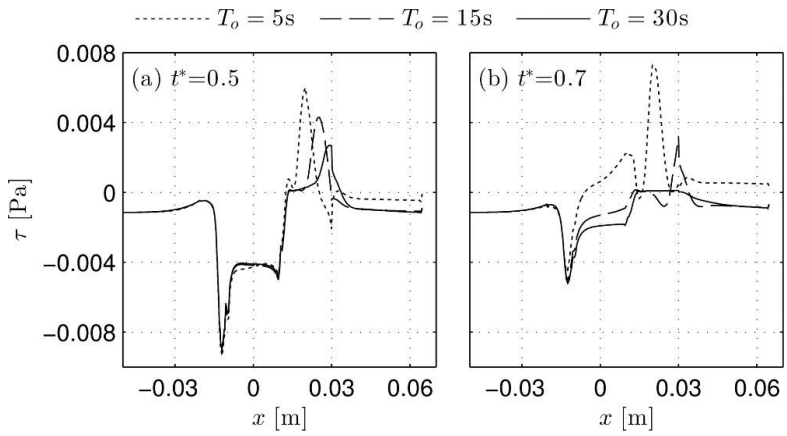

Figure 8. Wall shear stress distributions along the bottom wall in the deformable Y-channel

Figure 8(a) shows similar graph shapes of WSS distributions for all T_0 with the existence of one flow separation and reattachment region. T_0 = 5 s has the highest peak value and the reattachment region is formed at the right half of the indented wall (0<x< 0.03). In Figure 8(b), the longest region (0.015<*x*<0.06) with a small magnitude is found in the distribution of T_0 = 30 s. Contrarily, at T_0 = 5 s, the distribution shows the existence of the flow separation and reattachment at more than one regions (-0.01<x<0.015 and 0.02<x<0.029).

Conclusions

This present study focuses on the investigation of the effect of the wall oscillation period on the Newtonian fluid flow in the two types of branched channels. The governing equations of the fluid flow problem are defined in the ALE frame and solved by using the standard Galerkin technique. Three different values of the wall oscillation period are applied, and the small value of the oscillation period shows the faster motion of the indented wall in completing a one-time cycle. The fluid flow in the branches of the T-channel shows greater disturbance compared to Y-channel. The smallest value of the indentation oscillation period, i.e T_0 = 5 s; gives the most significant flow disturbance in branched channels. In the T-channel, the highly disturbed flow occurs at the smallest value of T_0, especially during the inward motion of the wall. In the Y-channel, though the disturbance is not as great as in the T-channel, the wavier core flow found in the parent channel for T_0 = 5 s; resulting in the formation of bigger vortices at the right lee of indentation and the upper armpit of the branch. In other words, the formation of a flow separation region is observed along the outer walls of both branches downstream of the armpits.

The present study limits the discussion by considering a single moving indented wall at the parent wall. The motion of the wall is prescribed as a hyperbolic function. Here, the interaction between the fluid and channel wall, and gravitational force are neglected. As this study is inspired by the interest in understanding the blood flow in a diseased vessel, future research should consider other new aspects in reducing the gap between this physiological flow and the simplified cases. For example, one might consider the use of an irregular shape of the indented wall, incorporating other forces or treating the fluid as a non-Newtonian. It is believed that the development and advancement of both computer technologies and numerical procedures will result in greater opportunities for researchers to better simulate the real problem.

Conflicts of Interest

The author(s) declare(s) that there is no conflict of interest regarding the publication of this paper.

Acknowledgment

Thank you to Universiti Teknologi MARA, Kelantan for providing sufficient facilities and moral support to us.

References

[1] Atobe, T. (2017). Stabilizing effects on 2D channel flow due to longitudinal wall oscillation. *AIP Conference Proceedings,* 1798. https://doi.org/10.1063/1.4972599.
[2] Ben-Mansour, R., Habib, M.A. & Shaik, A. Q. (2009). Modeling of fluid flow in a tube with a moving indentation. *Computers and Fluids*, *38*, 818-829.
[3] Bin Tan, Y. & Mustapha, N. (2018). Gravitational influences on micropolar blood flow in a bifurcated artery with mild stenosis. *International Journal of Advanced and Applied Sciences*, *5*, 24-32.
[4] Chen, H. Y. H. & Sheu, T. W. H. (2003). Finite-element simulation of incompressible fluid flow in an elastic vessel. *International Journal for Numerical Methods in Fluids*, *42*, 131-146.
[5] Damodaran, V., Rankin, G. W. & Zhang, C. (1999). Effect of a moving boundary on the pulsatile flow of incompressible fluid in a tube. *Computational Mechanics*, *23*, 20-32.
[6] Demirdžić, I. & Perić, M. (1990). Finite volume method for prediction of fluid flow in arbitrarily shaped domains with moving boundaries. *International Journal for Numerical Methods in Fluids*, *10*, 771-790.
[7] Engel, M. & Griebel, M. (2004). Flow simulation on moving boundary-fitted grids and application to fluid-structure interaction problems. *International Journal for Numerical Methods in Fluids*, *50*, 437-468.
[8] Förster, C. (2007). Robust methods for fluid-structure interaction with stabilised finite elements. Ph.D. Thesis. Universität Stuttgart.
[9] Lin, J. (2006). Pulsatile flow in a tube with a moving constriction. Ph.D. Thesis. The National University of Singapore.
[10] Lynn, N. S., Fox, V. G. & Ross, L. W. (1972). Computation of fluid-dynamical contributions to atherosclerosis at arterial bifurcations. *Biorheology*, *91*, 61-66.
[11] Md Yasin, R., Kasiman, E. H., Amin, N. S., Mohd Yassin, A. Y. & Hong, A. K. (2017). Numerical simulation of fluid flow in branched channels with a moving indentation. *Proceeding of International Conference on Mathematics, Statistics and Computing Technology (ICMSCT 2017)*. 16-17 October 2017. Kota Bharu, Malaysia. 1-12.
[12] Mohd Zainul Abidin, S. N. A. Jaafar, N. A. & Ismail, Z. (2021). Herschel-Bulkley model of blood flow through a stenosed artery with the effect of chemical reaction on solute dispersion. *Malaysian Journal of Fundamental and Applied Sciences, 17*, 457-474.
[13] Patel, S. S., Fischer, P., Min, M. & Tomboulides, A. (2019). A characteristic-based spectral element method for moving-domain problems. *Journal of Scientific Computing*, *79*, 10.1007/s10915-018-0876-6.
[14] Pedley, T. & Stephanoff, K. (1985). Flow along a channel with a time-dependent indentation in one wall: The generation of vorticity waves. *Journal of Fluid Mechanics*, *160*, 337-367.
[15] Ralph, M. E. & Pedley, T. J. (1988). Flow in a channel with a moving indentation. *Journal of Fluid Mechanics*, *190*, 87-112.
[16] Shixiong, X., Lin, J. & Qingwei, W. (2005). Numerical investigation of effect of rolling manipulation of traditional Chinese medical massage on blood flow. *Applied Mathematics and Mechanics*, *26*, 753-760.
[17] Skote, M., Mishra, M. and Wu, Y. (2019). Wall oscillation induced drag reduction zone in a turbulent boundary layer. *Flow Turbulence Combust*, *102*, 641-666.
[18] Sonawane, C. R., More, Y. & Pandey. A. (2022). Numerical simulation of unsteady channel flow with a moving indentation using solution dependent weighted least squares based gradients calculations over unstructured mesh. *Heat Transfer Engineering*, *43*, 300-313.
[19] Tomiyama, N. and Fukagata, K. (2013). Direct numerical simulation of drag reduction in a turbulent channel flow using spanwise traveling wave-like wall deformation. *AIP Conference Proceedings*, *25*. https://doi.org/10.1063/1.4826887.
[20] Yang, Y., Richter, T., Jager, W. and Neuss-Radu, M. (2016). An ALE approach to mechano-chemical processes in fluid-structure interactions. *Numerical Methods in Fluids*, *84*, 1990-220.
[21] Zain, N. M. & Ismail, Z. (2019). Hartmann and Reynolds numbers effects in the Newtonian blood flow of a bifurcated artery with an overlapping stenosis. *MATEMATIKA: Malaysian Journal of Industrial and Applied Mathematics*, *35*, 213-227.
[22] Zhao, Y. and Su, X. (2019). Chapter 13 - ALE FSI Model Validations and Applications. In Zhao, Y. & Su, X. *Computational fluid-structure interaction*. Academic Press. 409-480.